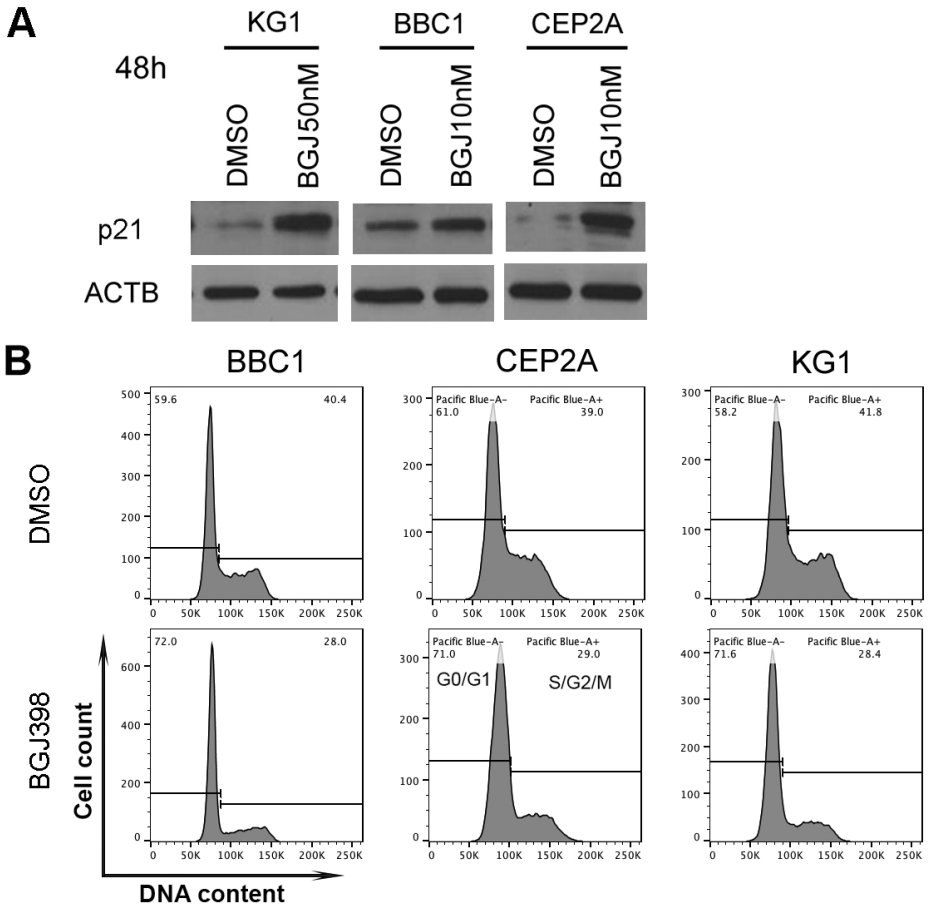

Supplemental figure 1. Western blot analysis of three SCLL cell lines treated with FGFR1 inhibitor BGJ398 at their IP_{50} (A) shows increased p21 levels in all cases suggesting impaired cell cycle progression. This suggestion is confirmed in flow cytometric analysis of cell cycle showing reduced levels of cells in S/G2/M in the inhibitor-treated cells (B).

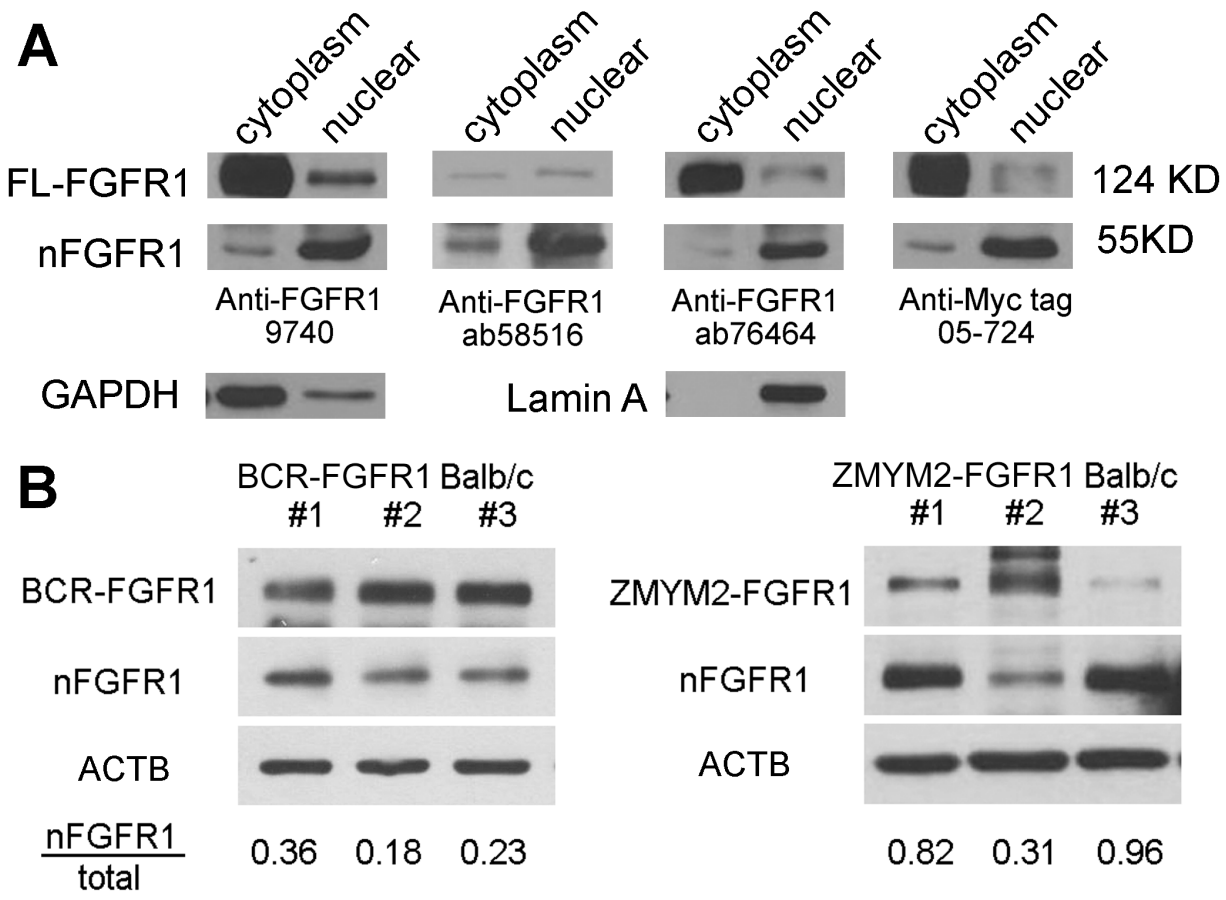

Supplemental figure 2: Analysis of FGFR1 antibodies in the BBC2 cell line. In this cell line the BCR-FGFR1 chimeric kinase resides predominantly in the cytoplasm, where the majority of the protein is phosphoactivated. When a Myc-tagged BCR-FGFR1 is expressed in BBC2 cells the cytoplasmic location of the full-length chimeric kinase and the nuclear location of the truncated FGFR1 kinase is confirmed (right). The 9740 anti-FGFR1 (Cell Signaling) and the ab76464 anti-FGFR1 (Abcam) antibodies recognize both the nuclear and the cytoplasmic variants of FGFR1 since they are both derived from the distal carboxy-terminus of the protein. Ab58516 (Abcam) was designed around the Y654 region of the FGFR1 kinase domain and was raised against a non-phosphorylated peptide. This antibody does not recognize the phosphorylated cytoplasmic form of the chimeric FGFR1 kinase but recognizes the nuclear truncated form, presumably because this derivative protein is unphosphorylated. When relative levels of the nuclear and cytoplasmic forms of FGFR1 were assayed in spleen cells from primary SCLL mouse models (B), although some minor heterogeneity is seen between animals, the relative levels of the nuclear form in three independent *in vivo* lines from the BCR-FGFR1 model were low (18-36%) consistent with a predominantly cytoplasmic location of this kinase in vitro. Similarly, in the ZMYM2-FGFR1 model, despite one outlier (31%), relative levels of the nuclear variant of FGFR1 were high (82-96%) consistent with the in vitro observation that this variant chimeric kinase is predominantly found in the nucleus.

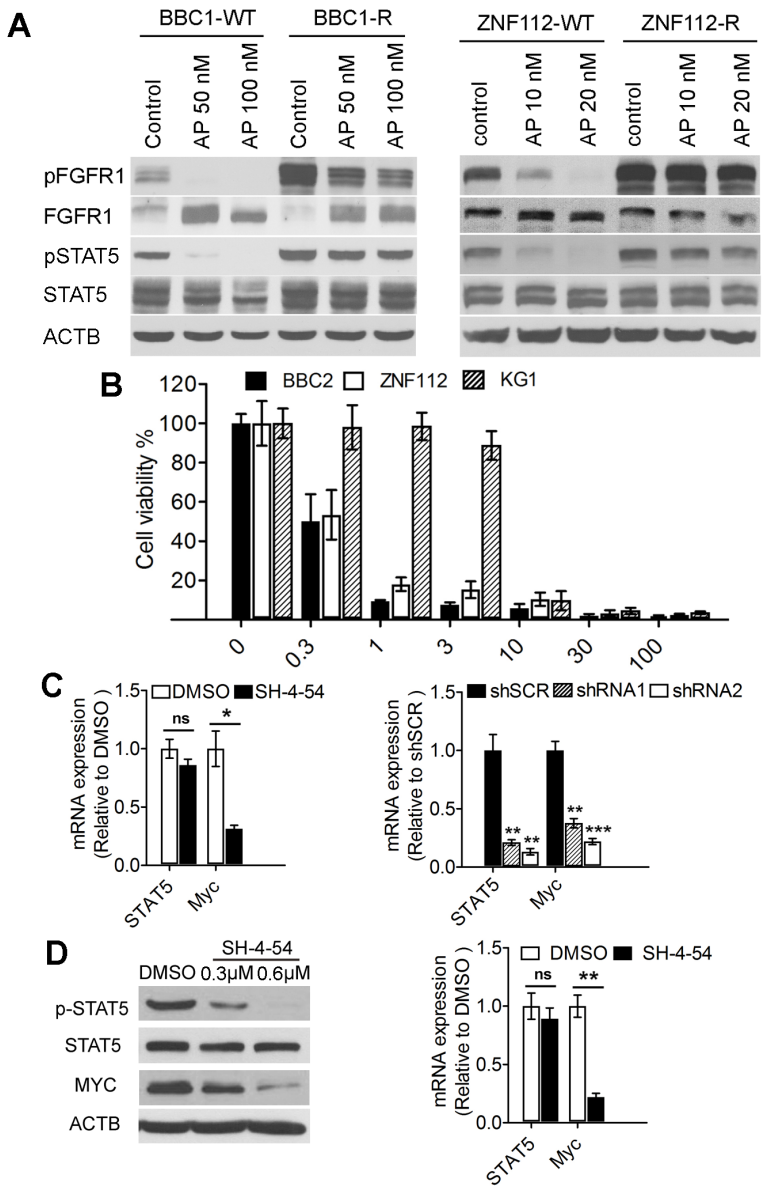

Supplemental figure S3. Analysis of SCLL cell lines BBC1-WT and ZNF112-WT (A) shows endogenous high-level activation of STAT5 (pSTAT5). Treatment of these cells with the FGFR1 inhibitor ponatinib (AP), at two different concentrations, suppresses FGFR1 activation and suppresses pSTAT5 activation. We recently described variants of these 2 cell lines that were resistant to ponatinib[33] and in these cell lines pFGFR1 and pSTAT5 activation is unaffected by the FGFR1 inhibitor, further demonstrating that STAT5 activation is dependent on activation of FGFR1. Titration of the STAT5 inhibitor SH-4-54 against SCLL cell lines that show either, predominantly cytoplasmic localization of FGFR1 (BBC2), predominantly nuclear localization (ZNF112) or presence in both compartments (KG1) shows that viability is reduced in all three cell lines at varying nanomolar concentrations (B). In BaF3 cells, RT-PCR analysis after SH-4-54 treatment suppresses Myc mRNA production but not STAT5. shRNA knockdown of STAT5 using two different shRNAs similarly leads to suppression of mRNA production for both genes (C). In the ZNF112 SCLL cell line, SH-4-54 also suppresses activation of STAT5 and Myc levels as a result of inhibition of Myc transcription (D).

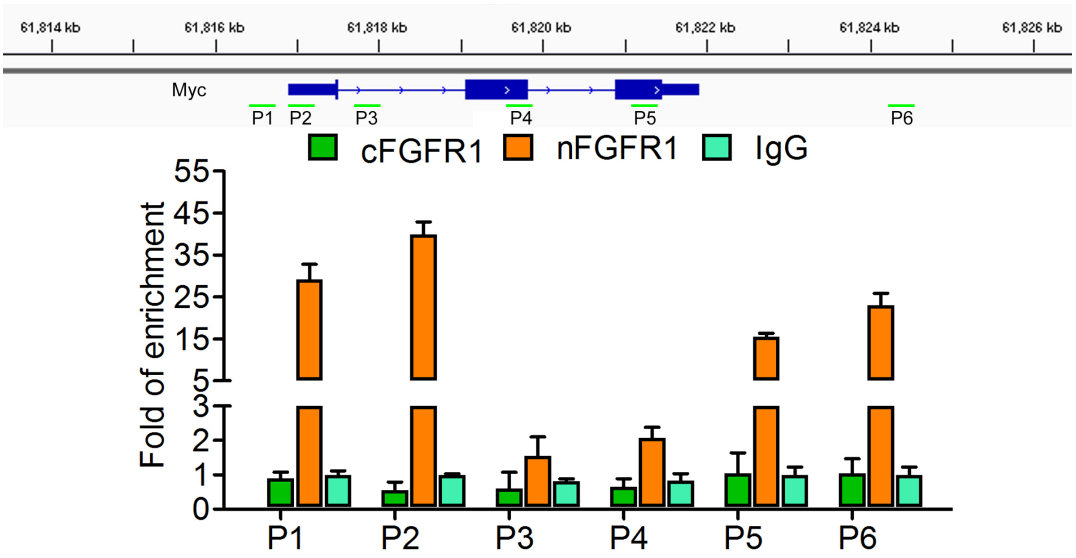

Supplementary figure S4. The ChIP scan for the Myc locus described in Figure 5 defines regions that bind nFGFR1. ChIP analysis for cFGFR1 and nFGFR1 binding to the various locations throughout the Myc locus demonstrates specific binding by nFGFR1 for P1, P2, P5, P6. Virtually no binding is seen in regions P3 and P4 as expected from the ChIP scan.

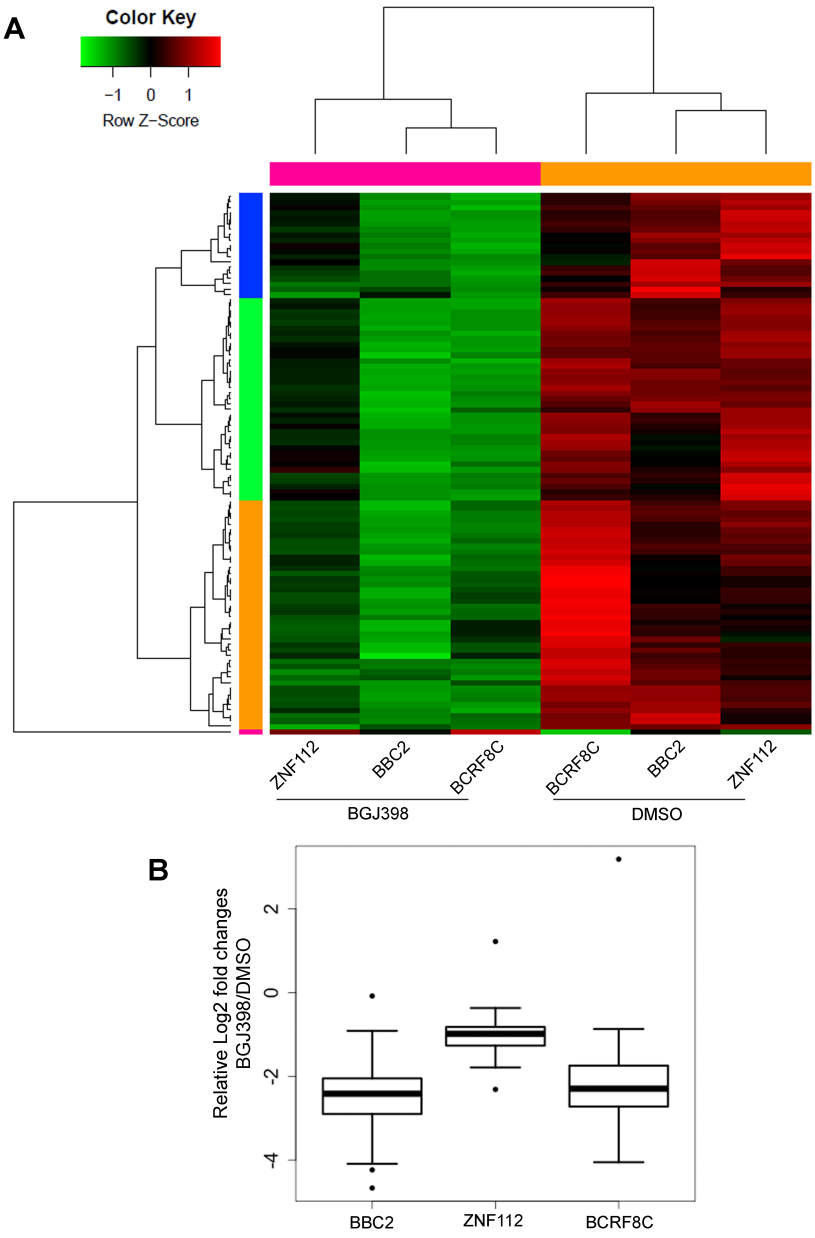

Supplemental figure S5. Data from ~130 genes known to be upregulated by MYC were analysed using hierarchical clustering (A) from RNASeq data comparing three cell lines expressing either BCR-FGFR1 (BCRF8C, BBC2) or ZMYM2-FGFR1 (ZNF112). Cells treated with DMSO (right 3 panels) show relatively high levels of expression of these genes compared with cells treated with BGJ398 (left 3 panels), where all of the genes are down regulated as a result of suppression of FGFR1 activation. The data is summarized in the box plots shown in (B) where the mean fold changes in the BGJ398 treated cells are 2-4 fold depending on the cell line.

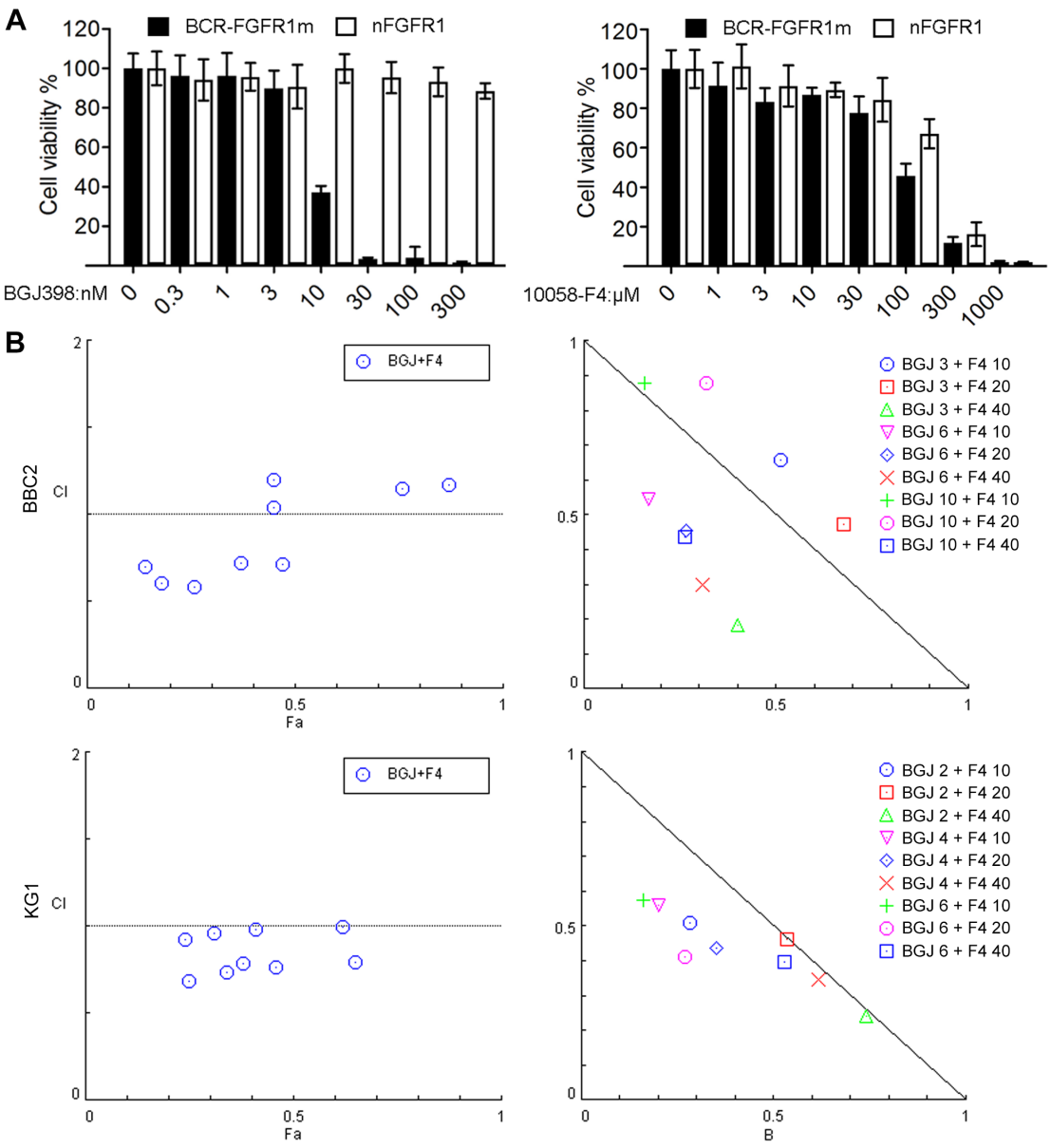

Supplementary figure S6. (A) Analysis of BaF3 cells over expressing either BCR-FGFR1m (cleavage resistant chimeric kinase) or the nFGFR1 (cleaved nuclear derivative) shows that there is a decrease in cell viability only in cells expressing the cytoplasmic derivative of FGFR1. This follows since BGJ398 suppresses activation of the cytoplasmic protein and not the nuclear derivative. In contrast (A, right), treatment of these cells with the MYC inhibitor decreases cell viability in both cell types. Isobologram analysis (B), following treatment of BBC2 and KG1 cells with different nanoMolar concentrations of BGJ398 and microMolar concentrations of 10058-F4, shows a synergistic effect following analysis of the combination index (CI) where values <1.0, indicate synergy) and typically at higher concentrations of both drugs. Experimental details and analysis were performed according to Chou T. Drug Combination Studies and Their Synergy Quantification Using the Chou-Talalay Method. Cancer Research.70; 440-446, 2010.